

# Graphene-Based Cathode Materials for Lithium-Ion Capacitors

Subjects: [Electrochemistry](#)

Contributor: Dong Sui

Lithium-ion capacitors (LICs) are attracting increasing attention because of their potential to bridge the electrochemical performance gap between batteries and supercapacitors. LICs are still impeded by their inferior energy density, which is mainly due to the low capacity of the cathode. Graphene-based nanomaterials have been recognized as one of the most promising cathodes for LICs due to their unique properties, and exciting progress has been achieved.

lithium-ion capacitors

graphene

graphene-based nanomaterials

capacitor-type electrodes

cathode materials

## 1. Introduction

Graphene, as a novel two-dimensional (2D) nanocarbon material, has many outstanding characteristics such as high theoretical SSA, astonishing electrical conductivity, tunable porosity and rich surface chemistry [\[1\]](#). It should be noted that graphene has comparable or even superior properties to other nanocarbon-based materials, making it an excellent candidate either as a high-performance active material or as an attractive flexible support to load other materials for applications in LIBs, SCs and hybrid devices [\[2\]\[3\]\[4\]\[5\]](#). In particular, graphene-based nanomaterials have been verified as desired capacitor-type cathodes for LICs [\[6\]\[7\]](#). According to the theoretical calculation, the specific capacitance of graphene can reach as high as  $550 \text{ F g}^{-1}$  based on the fully used SSA, significantly higher than that of commercial AC and other porous carbon materials [\[8\]](#). Moreover, the abundant edges, in-plane defects and large number of exposed surface atoms endow graphene with more electrochemical active sites for ion sorption/desorption [\[9\]](#). Thus, graphene and its composites demonstrate great appeal as capacitor-type electrodes with high capacity in LICs. As demonstrated in **Figure 1**, graphene or reduced graphene oxide can be directly used as active materials by rationally regulating the structure and surface chemistry. Simultaneously, they can also serve as excellent substrates or building blocks to form 3D porous composites, leading to improved electrical conductivity and/or SSA of the obtained composites. Exciting achievements of graphene-based cathodes in LICs have been made, strongly demonstrating their potential in enhancing the performance of capacitor-type cathodes [\[1\]\[6\]](#). Accordingly, some reviews about graphene-based anode materials for LICs have been reported [\[10\]\[7\]\[9\]\[11\]](#).

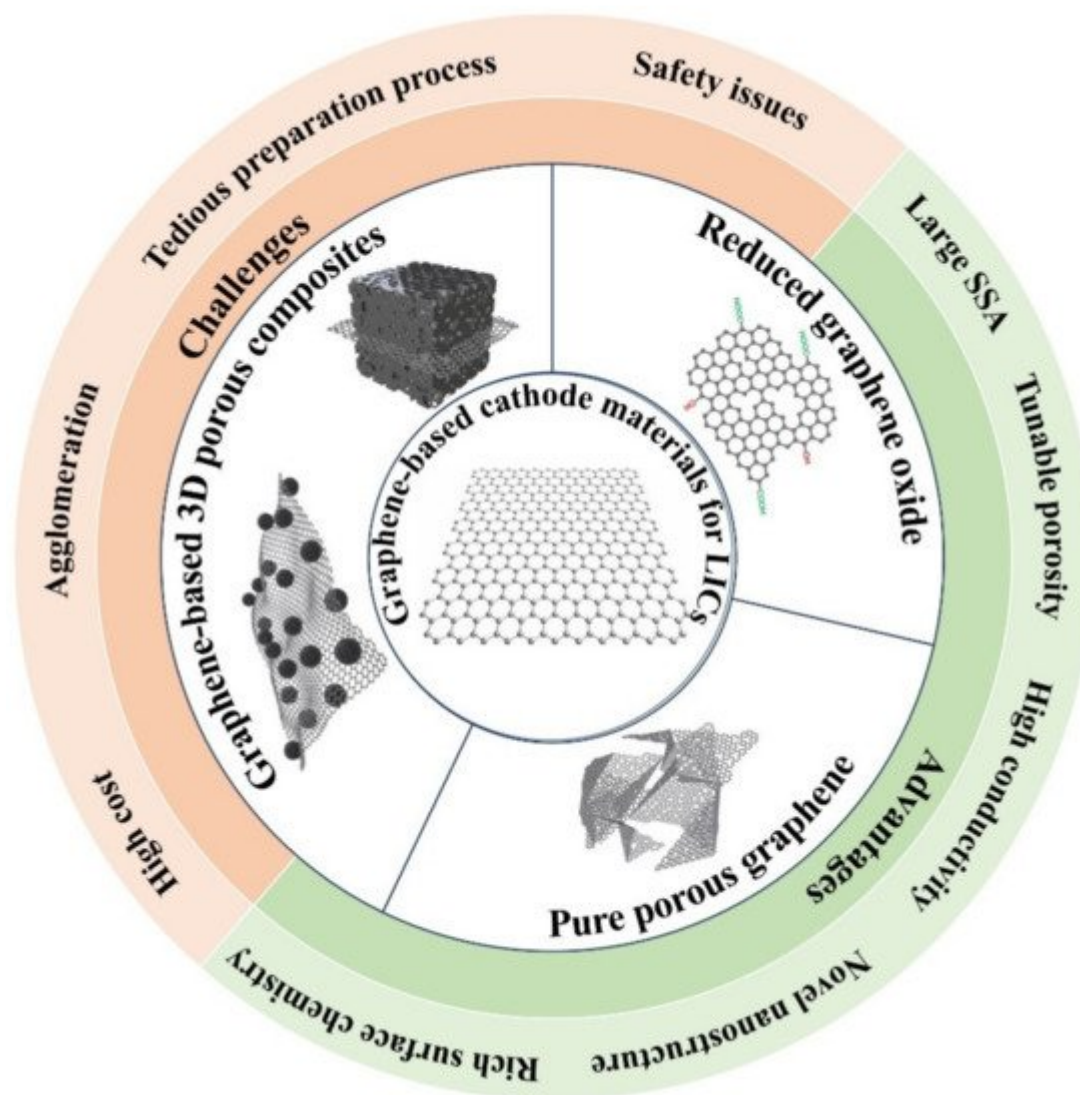


Figure 1. Typical graphene-based cathode materials for LICs and their advantages and the remaining challenges.

## 2. Reduced Graphene Oxide as a Cathode Material

### 2.1. Reduced Graphene Oxide

In the early stage, researchers usually applied reduced graphene oxide (rGO) as the capacitor-type active material for LICs because of its feasible fabrication procedure, controllable size and thickness and ease of handling [12]. In addition, the tunable surface functional groups provide extra capacitance via fast redox reaction [13]. For instance, Lee et al. reported an urea-reduced GO (URGO) cathode for LICs by treating GO with urea [14]. URGO shows a specific capacity of  $35 \text{ mAh g}^{-1}$ , which is about a 35% increase compared with conventional AC. Based on the mechanism analysis, the carbonyl groups in the amide groups are responsible for the enhanced capacity through binding with  $\text{Li}^+$  based on the enolization process ( $\text{N-C=O} + \text{Li}^+ + \text{e}^- \leftrightarrow \text{N-C-O-Li}$ ), which has also been observed in Li-organic batteries [15][16]. The as-fabricated LICs paired with the URGO cathode with a pre-lithiation graphite anode show an energy density of approximately  $106 \text{ Wh kg}^{-1}$  and power density of  $4200 \text{ W kg}^{-1}$  based on the mass of active materials, which is not only much higher than that of supercapacitors, but also superior to

hydrazine-reduced GO and AC-based devices. Another group assembled LICs with trigol-reduced GO (TRGO) as the cathode and LTO as the anode, and the LTO/TRGO LICs delivered a maximum energy density of  $45 \text{ Wh kg}^{-1}$  with a stable cycling performance of 5000 times [17]. The improved energy density can be ascribed to the high reversible capacity ( $58 \text{ mAh g}^{-1}$ ) of the as-synthesized TRGO, which is almost twice that of AC.

## 2.2. Three-Dimensional Reduced Graphene Oxide

The agglomeration of rGO can be largely suppressed by forming three-dimensional (3D) porous hydrogels or foams through self-assembly technology. Monolithic rGO hydrogel [18], porous graphene macroform (PGM) [19] and graphene grass [20] have been reported via a hydrothermal reduction combined with the freeze-drying process. The as-prepared samples have a 3D porous network structure, which can provide multidimensional transport pathways for electrons and electrolytes and minimize the transport distances between bulk electrodes and electrolytes [18][21]. This enables them to have high capacity and excellent power output, making them highly attractive cathode materials for LICs. Taking the formation of PGM for example, GO was partially reduced during hydrothermal treatment and self-assembled into graphene hydrogel through random cross-linking between flexible graphene sheets [19]. After removing the solvent by the freeze-drying process, the as-prepared PGM demonstrates a cylindrical morphology without obvious shrinkage (inset of Figure 2d). As displayed in Figure 2d, PGM has a continuous 3D porous framework with abundant micropores, mesopores and macropores, which could be verified from the  $\text{N}_2$  adsorption isotherm and pore size distribution (PSD) curves (Figure 2e,f). By paring with a LTO/C anode, the PGM-based LICs show an acceptable energy density of  $72 \text{ Wh kg}^{-1}$ , which still keeps  $40 \text{ Wh kg}^{-1}$  at a power density of  $8.3 \text{ kW kg}^{-1}$ .

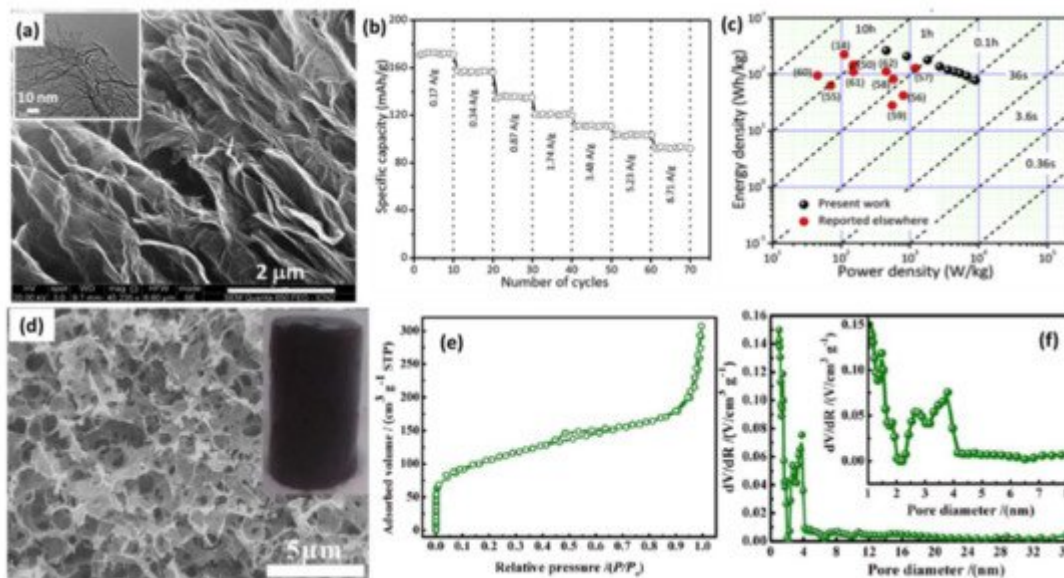


**Figure 2.** (a) FESEM of PRGO (inset shows TEM image); (b) Rate capability of PRGO; (c) Ragone plot for N-CNPipes//PRGO LIC and other devices. (Reprinted with permission from Ref. [22]. Copyright 2018 Elsevier.) (d) SEM image (The inset is the corresponding picture of the PGM), (e)  $\text{N}_2$  sorption isotherm, and (f) the pore size distribution curves of PGM. (Reprinted with permission from Ref. [19]. Copyright 2015 Elsevier.)

## 3. Pure Porous Graphene as a Cathode Material

### 3.1. Porous Graphene Prepared with Template

Typically, the methodology combining chemical vapor deposition (CVD) and hard template is applied to prepare porous graphene materials with high conductivity and large SSA [23][24]. For example, Ma et al. designed S,N-codoped mesoporous graphene (SNMG) based on the CVD method using heavy MgO flakes as a solid template [25]. As displayed in **Figure 3a**, graphene firstly grew on the surface and pores of MgO thin lamellas by  $\text{CH}_4$  catalytic deposition in a fluidized-bed reactor, and then the templates were removed by acid washing to obtain few-layered mesoporous graphene (MG), followed by annealing with thiourea to form the final products. The as-prepared SNMG exhibits a highly porous structure with pore size in the range of 2–10 nm, which is clearly demonstrated in the TEM image (**Figure 3b**) and PSD (**Figure 3c**). The interconnected and controllable mesopores combined with sulfur and nitrogen co-doping endow the SNMG cathode with outstanding rate capability. A reversible capacity of  $112 \text{ mAh g}^{-1}$  can be achieved at a current density of  $0.5 \text{ A g}^{-1}$  and still retain  $92 \text{ mAh g}^{-1}$  at  $5 \text{ A g}^{-1}$ , which is much better than that of MG and AC (**Figure 3d**). In addition, SNMG shows excellent cycling stability with no obvious capacity decay after 2500 cycles (**Figure 3e**).

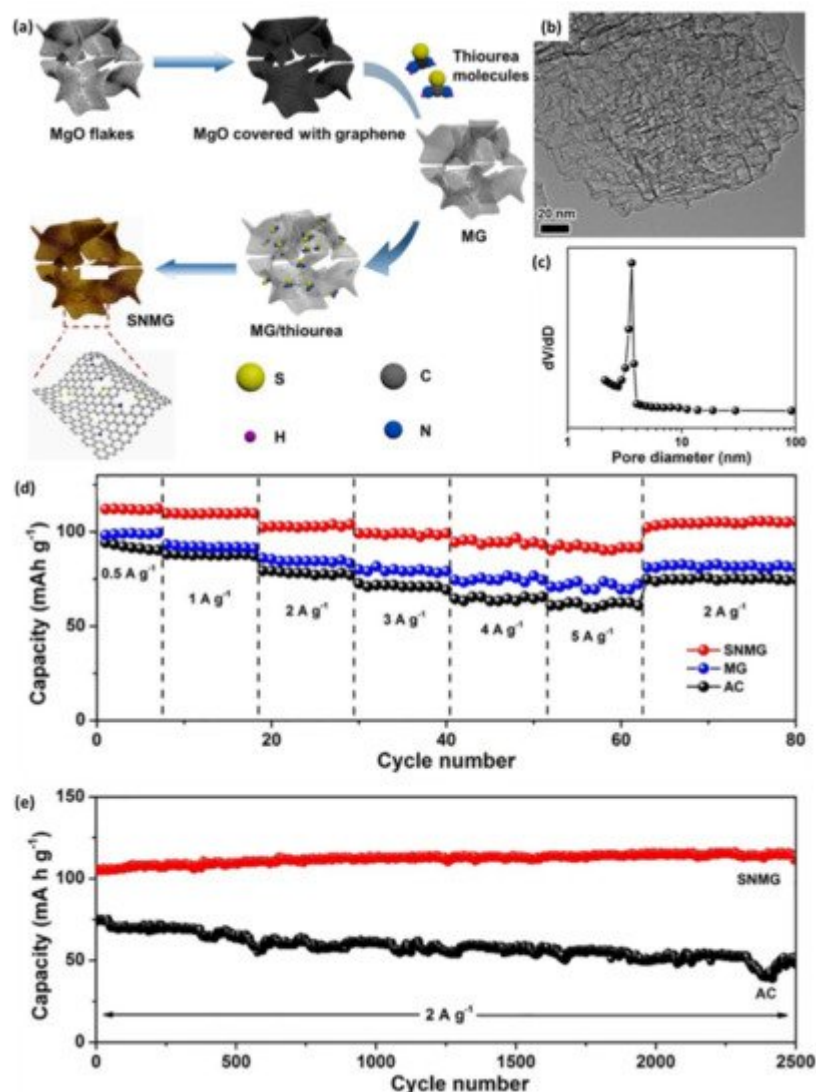


**Figure 3.** (a) Schematic of the preparation process of SNMG; (b) TEM image and (c) PSD of SNMG; (d) Rate capability of SNMG, MG and AC; (e) Cycling stability of SNMG and AC. (Reprinted with permission from Ref. [25]. Copyright 2018 Wiley-VCH.).

### 3.2. Porous Graphene Prepared by Chemical Activation

Chemical activation is an effective and feasible strategy to produce porous carbon materials with high SSA and large pore volume, which is commonly used in the preparation of commercial AC [26]. The activation process with KOH as an activation agent is proposed to follow the below reactions [27]:



The activation procedure starts from the reaction of KOH with carbon and then the decomposition of  $\text{K}_2\text{CO}_3$  and/or reactions of  $\text{K}_2\text{CO}_3/\text{K}_2\text{O}/\text{CO}_2$  with carbon, creating a porous carbon material. Ruoff et al. reported “activated microwave expanded graphite oxide” (a-MEGO) by irradiating GO in a microwave oven in combination with chemical activation (Figure 4a) [28]. As exhibited in Figure 4b–d, a-MEGO possesses a dense pore structure with a continuous 3D network of highly curved and predominantly atom-thick walls. The extraordinarily high SSA ( $3100 \text{ m}^2 \text{ g}^{-1}$ ) coupled with a continuous 3D network of extremely small size pores (ranging from  $<1 \text{ nm}$  to  $10 \text{ nm}$ ) endowed a-MEGO with a high specific capacity ( $125 \text{ mAh g}^{-1}$ ) [29]. Specifically, the graphite//a-MEGO LIC yielded an energy density of  $147.8$  and  $53.2 \text{ Wh kg}^{-1}$  at an operating potential of  $4 \text{ V}$  based on the active materials and the packaged full cell, respectively. Inspired by the pioneering work of Ruoff’s group, pure graphene-based porous materials with high SSA and large pore volume were prepared by the chemical activation of reduced GO foam or hydrogel and used as capacitor-type electrodes for LICs [30][31]. For example, porous graphene (PG) reported by Yang et al. showed a highly crumpled and porous structure after hydrothermal reaction and KOH treatment (Figure 4e) [31]. Specifically, PG has a surface area of  $2103 \text{ m}^2 \text{ g}^{-1}$  and pore volume of  $1.8 \text{ cm}^3 \text{ g}^{-1}$  with PSD centered at about  $5 \text{ nm}$  (Figure 4f). Consequently, the interpenetrated pores and excellent conductivity endowed PG with outstanding electrochemical performance, such as excellent rate capability and good long-term stability (Figure 4g–h).

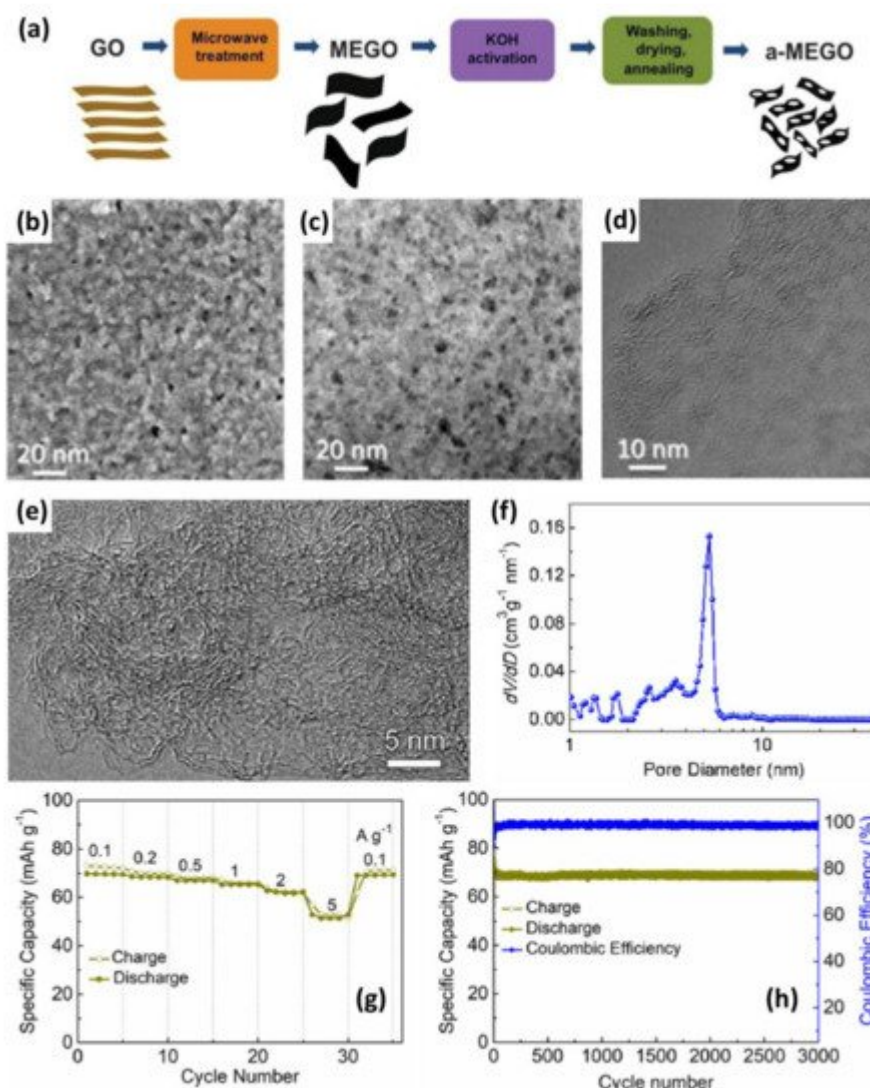


**Figure 4.** (a) Schematic of preparation of a-MEGO. (b) High-resolution SEM, (c) annular dark field STEM and (d) high-resolution TEM images of a-MEGO. (Reprinted with permission from Ref. [28]. Copyright 2011 American Association for the Advancement of Science.) (e) High-resolution TEM images and (f) pore size distribution curve of PG; (g) Rate capability and (h) cycling stability of PG. (Reprinted with permission from Ref. [31]. Copyright 2020 Elsevier.).

### 3.3. Porous Graphene Prepared by Other Methods

Catalytic carbon gasification is another method to prepare porous carbon materials. For example, Jeong et al. fabricated holey graphene (HG) with abundant in-plane pores using this method [32]. The synthesis process of HG is displayed in **Figure 5a**. Firstly, catalytic metal oxide ( $\text{SnO}_2$ ) nanoparticles were uniformly deposited onto the graphene oxide sheets via an aqueous-solution-based regular deposition process. Then, the  $\text{SnO}_2/\text{GO}$  suspension was spray-dried to obtain a spherical composite, which was heated to induce the selective decomposition of the graphene adjacent to the  $\text{SnO}_2$  nanoparticles. It is noteworthy that the temperature should be carefully adjusted to be lower than the carbon combustion temperature in the catalytic carbon gasification process. Finally, the spherical  $\text{SnO}_2/\text{rGO}$  was refluxed in HI to etch the catalysts and to reduce GO. The as-prepared HG has a spherical

morphology and porous structure with rich in-plane holes of about 5 nm corresponding to the metal oxide size (Figure 5b). The  $N_2$  adsorption/desorption isotherm of HG indicates the existence of micropores and smaller mesopores (Figure 5c). This result can be further verified by the pore size distribution curve (inset of Figure 5c), which demonstrates that HG has micropores of 1 nm and some mesopores of 2–6 nm. Due to its highly porous structure, HG shows much higher capacity than that of crumpled rGO prepared from GO by heat treatment (Figure 5d). As expected, LICs constructed using HG as a cathode and LTO/HG as an anode delivered a maximum energy density of  $117.3 \text{ Wh kg}^{-1}$ , which still remains at  $43.1 \text{ Wh kg}^{-1}$  even at an extremely high power density of  $19.7 \text{ kW kg}^{-1}$  (Figure 5e). The outstanding electrochemical performance can be attributed to the good match of capacity and rate between the capacitor-type cathode and the battery-type anode.

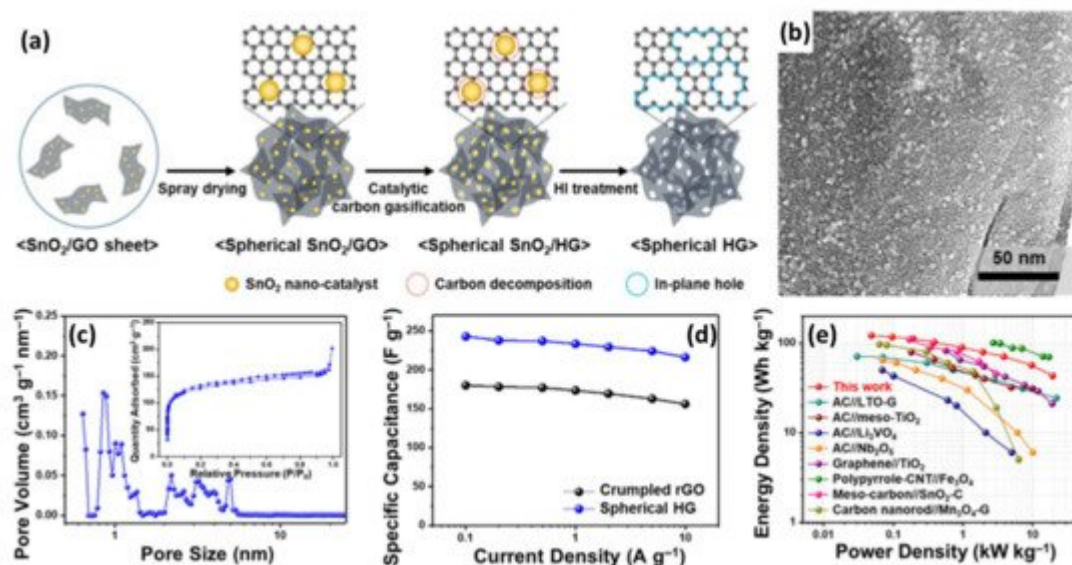


**Figure 5.** (a) Schematic of spherical HG preparation using catalytic carbon gasification; (b) TEM image and (c)  $N_2$  adsorption/desorption isotherm (inset) and pore size distribution of spherical HG; (d) Rate capabilities for spherical HG and crumpled rGO; (e) Ragone plots for the LICs composed of spherical HG and spherical LTO/HG composite. (Reprinted with permission from Ref. [32]. Copyright 2019 Elsevier.).

## 4. Graphene-Based 3D Composites as Cathode Materials

### 4.1. Graphene@Porous Carbon-Based 3D Composites

#### 4.1.1. Graphene@Non-Doped Porous Carbon 3D Composites

Chen's group designed a simple, low-cost and green but very efficient approach to prepare 3D graphene-based porous materials (3DGraphene) with GO sheets and biomass or polymers (such as phenolic resin, sucrose and polyvinyl alcohol) using standard industry steps of in situ hydrothermal polymerization/carbonization and KOH activation (Figure 6a) [33]. The graphene sheets derived from GO could effectively block the stacking of the AC precursor generated from the matrix carbon sources during the hydrothermal reaction, and thus thinner and smaller AC particles are formed with more pores in the next chemical activation step. The activated products with the

optimized ratio show a sponge-like morphology, highly porous structure and consist of mainly defected/wrinkled single-layer graphene sheets in the dimensional size of a few nanometers (**Figure 6b–d**). All the 3DGraphene materials have an ultrahigh SSA of over  $3000 \text{ m}^2 \text{ g}^{-1}$  and excellent bulk conductivity (up to  $303 \text{ S m}^{-1}$ ) because of the introduction of graphene. Taking the sucrose-based 3DGraphene, for example, it achieves an ultrahigh SSA of  $3355 \text{ m}^2 \text{ g}^{-1}$  with a well-controlled pore size of primarily 2–6 nm for the samples of optimized ratio (**Figure 6e,f**), making it an ideal capacitor-type material for LICs. By integrating it with an  $\text{Fe}_3\text{O}_4$ /graphene anode, the as-prepared LICs demonstrate a maximum energy density and power density of  $204 \text{ Wh kg}^{-1}$  at  $4600 \text{ W kg}^{-1}$ , respectively, which is much higher than the 3DGraphene//3DGraphene symmetric supercapacitor (**Figure 6g**) [34].

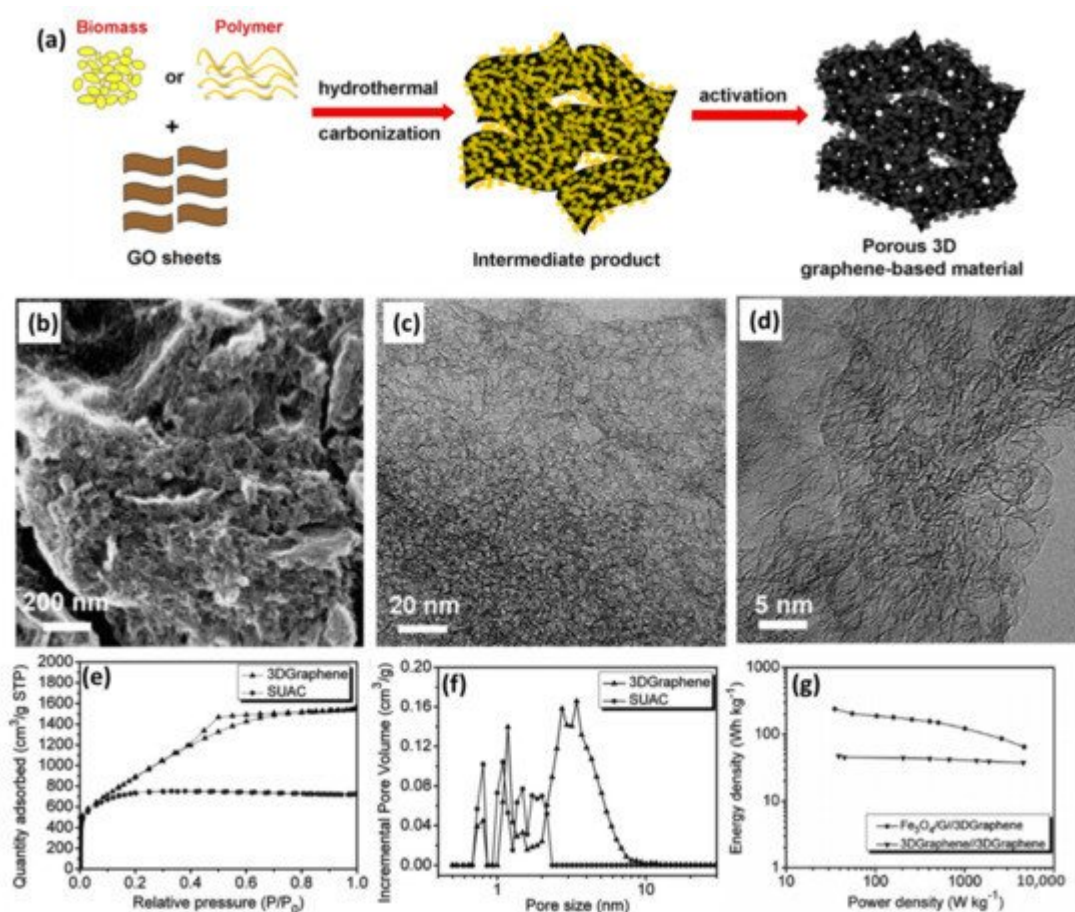


**Figure 6.** (a) Schematic of synthesizing porous 3D graphene-based materials; (b) SEM and (c,d) TEM images of 3DGraphene. (Reprinted with permission from Ref. [33]. Copyright 2013 Springer) (e)  $\text{N}_2$  adsorption–desorption isotherms and (f) pore size distribution of sucrose-based 3DGraphene and pure sucrose-based AC as contrast; (g) Ragone plots of the  $\text{Fe}_3\text{O}_4/\text{G}/3\text{DGraphene}$  LICs and 3DGraphene//3DGraphene supercapacitors. (Reprinted with permission from Ref. [34]. Copyright 2013 Royal Society of Chemistry.).

#### 4.1.2. Graphene@Doped Porous Carbon 3D Composites

Although the capacity of porous graphene-based cathodes is largely improved compared with AC, there is still a long way to go to meet the ever-growing demand of materials with high capacity. Several simple but effective methods have been adopted to further increase the capacity of capacitor-type electrodes, such as designing novel

structures and/or doping with heteroatoms [35][36][37]. Li et al. reported a sandwich-like graphene@hierarchical meso-/micro-porous carbon (G@HMMC) with functional oxygen containing groups through a facile carbonization and chemical activation procedure (Figure 7a) [38]. As displayed by the SEM and TEM images in Figure 7b,c, G@HMMC is composed of wrinkled multilayer nanosheets with a sandwich-like porous structure and the 2D structure of graphene is well retained after activation. The hierarchical porous structure of G@HMMC is consistent with the PSD characterization, which is mainly meso-/micropores (Figure 7d). For the optimized sample (G@HMMC850), the highest SSA of 2674.6 m<sup>2</sup> g<sup>-1</sup> and the largest pore volume of 1.67 cm<sup>3</sup> g<sup>-1</sup> were obtained (Figure 7e). Coupling with a moderate oxygen content that could provide extra capacity by fast redox reaction and increase the wettability with electrolytes, G@HMMC850 delivers a high specific capacity of 112 mAh g<sup>-1</sup> at 0.2 A g<sup>-1</sup> and remains around 90 mAh g<sup>-1</sup> at 8.0 A g<sup>-1</sup>, making it an advanced capacitor-type material (Figure 7f). As expected, LICs using G@HMMC850 as a cathode achieve an ultrahigh energy density of 233.3 Wh kg<sup>-1</sup> at 450.4 W kg<sup>-1</sup>, which still keeps 143.8 Wh kg<sup>-1</sup> at an extremely high power density of 15.7 kW kg<sup>-1</sup> (Figure 7g).

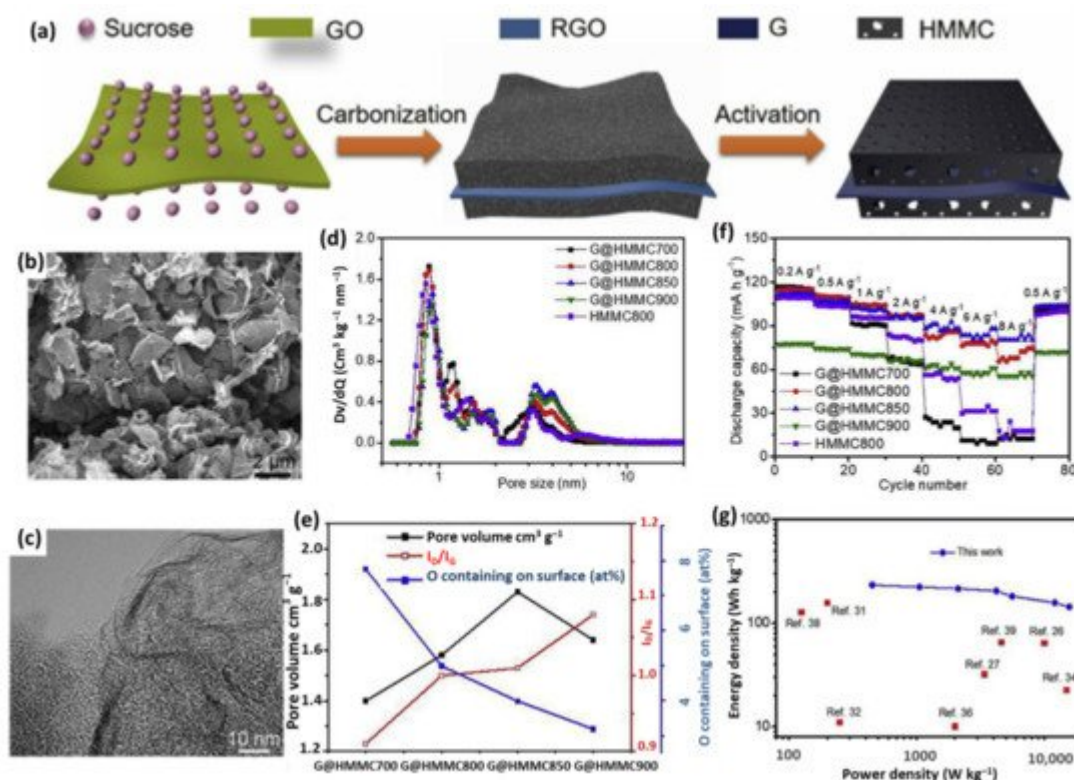


**Figure 7.** (a) Schematic of fabrication process of G@HMMC; (b) SEM and (c) TEM images of G@HMMC850; (d) PSD, (e) the pore volume, O contained on surface, and  $I_G/I_D$  values and (f) rate performances of G@HMMC materials; (g) Ragone plot of G@HMMC-based LIC compared with other works. (Reprinted with permission from Ref. [38]. Copyright 2018 Elsevier.).

## 4.2. Graphene/Nanostructured Material 3D Composites

In the previous reports, conductive extra spacers (such as CNTs, ACs or conductive polymers, etc.) were usually introduced to prevent the restack of graphene-based materials by forming 3D composites, which leads to high SSA and/or electrical conductivity, and thus excellent specific capacitance and rate capability could be obtained [8][39].

Similar strategies have been adopted to prepare high-performance capacitor-type electrodes for LICs [40][41][42][43]. In such cases, the serious aggregation or restacking of graphene could be suppressed so that the effective SSA could be enhanced. On the other hand, the spacers could also provide additional capacity through ion adsorption/desorption. For example, Wang et al. synthesized a durable and self-supporting graphene foam (GF) by microwave reduction of a polyvinyl pyrrolidone-stabilized GO/carboxylic CNT composite (**Figure 8a**) [44]. As displayed in **Figure 8b**, a reticulum-like porous structure of the as-prepared GF was generated after the rapid reduction. More importantly, CNTs serving as the spacer not only effectively prevent the restacking of reduced GO but also form a 3D conductive network. Benefiting from the highly porous structure and excellent electrical conductivity of GF, the assembled LICs with a porous LTO on CNT film as an anode exhibited an energy density of  $101.8 \text{ Wh kg}^{-1}$  (at a power density of  $436.1 \text{ W kg}^{-1}$ ) and a capacitance retention of 84.8% after 5000 cycles. Sun et al. fabricated a single carbon nanotube (SWCNT) and graphene composite (SG) by inserting the SWCNT into the space between the graphene nanosheets [45]. As shown in the SEM and TEM images of the SG composite (**Figure 8c,d**), SWCNTs were successfully inserted and homogeneously distributed between the graphene layers, which resulted in a highly 3D porous structure and an improved overall electrical conductivity. Therefore, the SG composite can effectively prevent the restacking of graphene and provide sufficient active sites for ion adsorption/desorption, making it a favorable capacitor-type electrode for LICs.

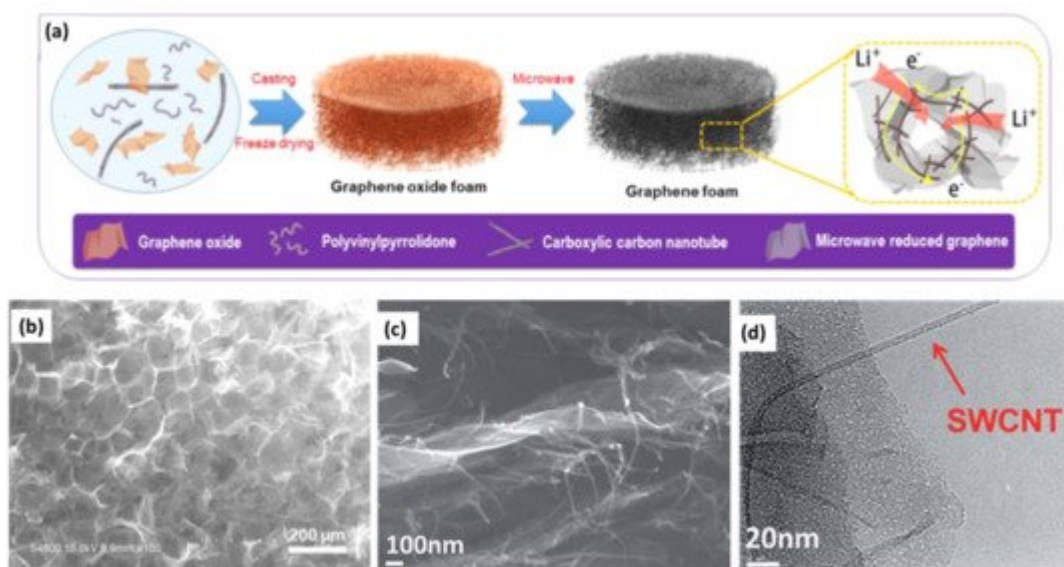


**Figure 8.** (a) The schematic illustration of preparation of GF and (b) SEM image of GF. (Reprinted with permission from Ref. [44]. Copyright 2020 Elsevier.) (c) SEM and (d) TEM images of SG. (Reprinted with permission from Ref. [45]. Copyright 2017 Royal Society of Chemistry.)

### 4.3. High-Density Graphene-Based 3D Composites

Commonly, carbon-based cathode materials suffer from low packing/tap density because of their highly porous structure, and this is more serious for nanostructured carbon materials (e.g., graphene or CNTs), which always leads to inferior volumetric energy density [46]. Therefore, developing materials with high packing/tap density is of great significance for fabricating high energy density LICs. For instance, Huang et al. demonstrated a novel

nitrogen-enriched mesoporous carbon nanosphere/graphene (N-GMCS) composite with high packing density [47]. The preparation process of N-GMCS includes the following steps (Figure 9a). Initially, mesoporous carbon nanospheres were formed on the graphene oxide substrate through in situ polymerization of phenolic resin under a hydrothermal reaction and subsequent carbonization. After the intermediate product was further activated by KOH and doped with abundant nitrogen functionality by NH<sub>3</sub> treatment, the final product was obtained. N-GMCS possesses a hierarchical porous structure, 3D conductive network as well as high packing density (0.6 g cm<sup>-3</sup>), making it a promising capacitor-type electrode for high-energy devices. As expected, LICs with N-GMCS as the cathode delivered maximum energy and power densities of 80 Wh kg<sup>-1</sup> and 352 kW kg<sup>-1</sup>, respectively (corresponding to 66.7 Wh L<sup>-1</sup> and 292 kW L<sup>-1</sup>) (Figure 9b).

Recently, Yang and coworkers designed a highly dense but porous activated carbon/graphene (AC/G) composite as the capacitor-type cathode for high gravimetric/volumetric energy density LICs [48]. The typical preparation of AC/G composites involves a process of hydrothermal reaction, capillary drying and high-temperature annealing (Figure 9c). As clearly demonstrated in the SEM images and photographs in Figure 9d, the volume of AC/G hydrogel and the voids between AC microparticles are significantly reduced to obtain a dense AC/G monolith after the capillary drying process, illustrating that a compact microstructure is formed. By contrast, the AC/G-FD monolith prepared through the freeze-drying process keeps almost the same size and appearance as the intermediate hydrogel with a loose morphology (Figure 9e), which strongly shows the advantages of capillary drying in preparing high-density electrodes. The highly dense but porous characteristic of AC/G composites can be verified by the results of SSA and electrode density (Figure 9f). For example, AC/G-57 has an SSA of 1402 m<sup>2</sup> g<sup>-1</sup> and its electrode density is still as high as 0.71 g cm<sup>-3</sup>, which is around 173% of that of AC. Hence, although AC/G-57 shows relatively lower gravimetric specific capacity compared with pristine AC, it has the largest volumetric specific capacity of 45 mAh cm<sup>-3</sup>, which is 137% of AC and 147% of HPGM, respectively (Figure 9g). Furthermore, AC/G-57 shows a higher capacity than that of AC, especially at high current density, which can be attributed to the fast and effective ion and electron conductive network formed by the 3D graphene skeleton (Figure 9h).

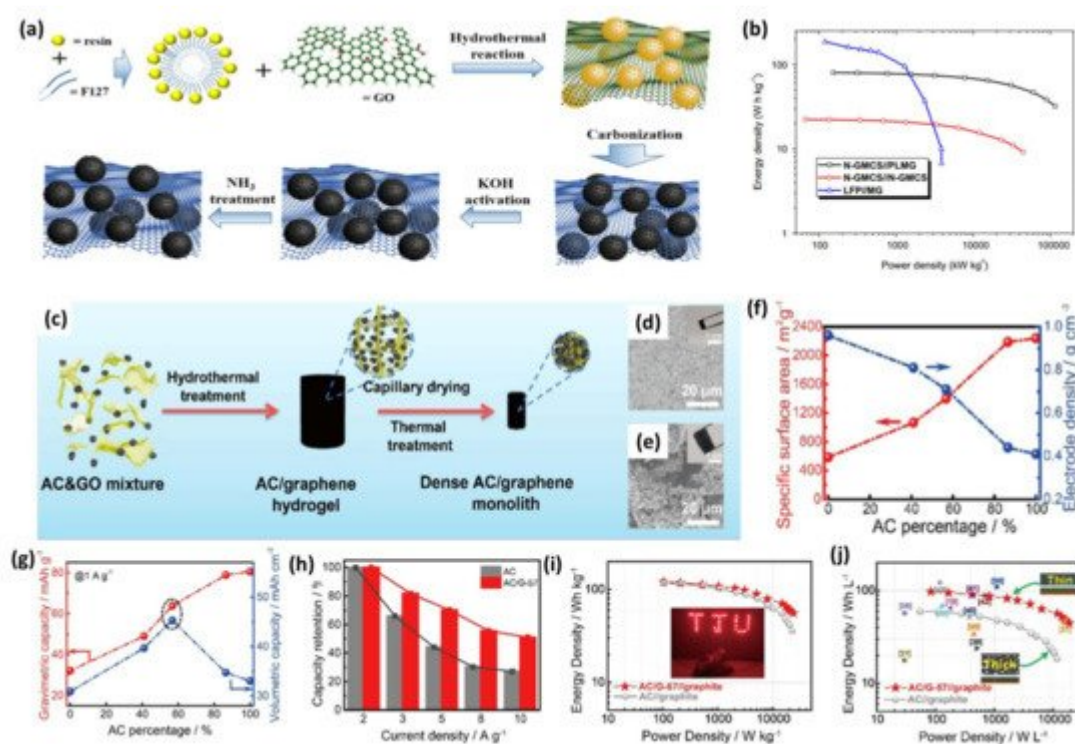


**Figure 9.** (a) Schematic of the synthesis of the NGMCS nanocomposite; (b) TEM image of the N-GMCS nanocomposite. (Reprinted with permission from Ref. [47]. Copyright 2015 Elsevier.) (c) Schematic of the AC/G composite monolith fabrication process; SEM images of (d) the capillary drying-induced dense AC/G monolith and (e) the freeze-drying-induced AC/G hydrogel; (f) The SSA and electrode density variations of the AC/G composites with the percentage of AC; (g) The relationship between the gravimetric/volumetric capacity and the percentage of AC in the AC/G composites; (h) Comparison of the capacity retention of pure AC and AC/G-57 electrodes at various current densities; Ragone plot of the AC/G-57//graphite LIC compared with the AC//graphite LIC based on (i) mass and (j) volume. (Reprinted with permission from Ref. [48]. Copyright 2019 Elsevier.).

## 5. Outlook

the following several aspects should be considered to overcome the present challenges and to realize the commercialization of LICs:

- (1) High-capacity capacitor-type materials are urgently needed. To match the high capacity of battery-type anodes, developing cathode materials with improved capacity is the top priority. The cathode stores energy through a physical adsorption/desorption process at the electrolyte/electrode interface, which leads to a fast charge/discharge rate. On the other hand, the non-Faradaic energy storage mechanism also results in low capacity because it is critically influenced by the SSA. A high SSA could provide more active sites for ion adsorption and, to a certain extent, the capacity is raised with the increase in the SSA. However, it should be pointed out that not all the surface can be accessible by the electrolyte ions [49]. Therefore, the morphology, pore size and surface chemistry of graphene-based cathode materials should be carefully regulated to increase the effective surface area and in turn enhance their capacity. In addition, heteroatom doping and porosity

engineering should also receive enough attention to obtain high-capacity and high-rate capacitor-type cathodes. Doping can not only provide extra capacity by fast redox reactions but enhance the electrical conductivity, while rational and tunable porosity is beneficial for the electrolyte ions' diffusion, together resulting in excellent rate capability.

- (2) The preparation of graphene-based cathode materials at low cost is one of the critical factors for large-scale applications. Although pure graphene-based porous materials can serve as outstanding capacitor-type electrodes due to their high electrical conductivity and large SSA, the high cost impedes their further commercial utilization. Forming composites with other materials is a facile but feasible method to solve this problem, such as biomass or polymer/graphene hydrogel-derived graphene-based 3D porous materials initially proposed by Chen's group [33]. In such cases, the overall cost of the cathode materials can be largely reduced but the high conductivity and porous structure can be kept.
- (3) Developing battery-type materials with a high rate and long-term stability is another big challenge but imperative issue. High-capacity anodes ensure the high energy of the full cell. However, the high energy density of state-of-the-art LICs could only be realized at the cost of low power output because of the sluggish redox reaction and/or inferior electrical conductivity of battery-type anodes. Hence, designing nanostructured materials with tunable porosity and compositing with highly conductive materials are always applied to achieve high-rate anodes. These strategies could help to reduce the capacity and kinetics imbalances between the cathode and anode, leading to improved energy and power densities [50]. With the booming of lithium metal batteries, Li metal anodes have also been applied as the battery-type electrode to develop high-energy LICs [48][51]. In this circumstance, elaborate surface coating or electrolyte regulation is needed to suppress lithium dendrite growth to avoid safety accidents [52][53].
- (4) The volumetric performance of graphene-based materials should receive more attention for commercial applications. Graphene-based cathode materials have shown enhanced gravimetric capacity compared with commercial AC. However, their large SSA and highly porous structure result in a low taping density and consequently low volumetric energy density, which is a big obstacle for practical utilization. In addition, more binders and solvents are needed in the electrode fabrication process because of the highly porous nanostructured carbon materials, increasing the manufacturing cost and decreasing the energy density. Thus, the porosity and taping density should be well balanced. To achieve high volumetric energy density at a low cost, future research can focus on forming graphene-based 3D composites by using capillary drying or rapid drying processes [48][54].
- (5) Advanced electrolytes with a wide working voltage and high safety are also needed. Currently, typical LICs commonly adopt organic electrolytes to achieve a high operation voltage. However, they suffer from safety issues associated with volatility, flammability and toxicity. Hence, other novel electrolytes have been explored. For example, ionic liquids are regarded as a promising alternative to the organic electrolyte owing to their large working voltage, high conductivity and excellent thermal stability without risk of catching fire [49][55]. Recently, "Water-in-Salt" electrolytes have drawn tremendous interest as they inherit the safety advantage of aqueous electrolytes while keeping the high working voltage of organic electrolytes [56][57][58][59].

- (6) The decomposition of electrolytes should not be ignored. Generally, electrolyte decomposition on the cathode and anode takes place during the charge/discharge process, especially at a high working voltage, resulting in gas emission, impedance increase and low energy conversion efficiency. At the anode side, this phenomenon can be largely restrained by forming a stable solid–electrolyte interface (SEI) during the first several cycles. However, an effective strategy to suppress the electrolyte decomposition at the cathode side is still absent [60]. Fortunately, Li et al. proposed a preliminary electrochemical coating process to form a well-formed protective layer on a graphene-based cathode [61]. The protective layer could block the electron flow from the cathode to the electrolyte and thus terminate the decomposition. This may be a possible and promising solution to obtain high-voltage and long-durability LICs. Furthermore, some in situ and ex situ characterization technologies could be applied to investigate the decomposition mechanism of electrolytes, the degradation and/or evolution of the electrode surface and electrode/electrolyte interface and the composition of decomposed products [62][63][64]. It is expected that these in situ and ex situ tools will help us to understand the beneath decomposition mechanism and find an effective protection method.
- (7) Besides the above discussion, other critical issues should also be solved before industrial-level production and widespread applications. First of all, feasible pre-lithiation technology should be developed because the anode, especially nanostructured materials with a large SSA and rich porosity, would consume a large amount of lithium ions when forming a stable SEI [65][66]. Well-controlled pre-lithiation could largely improve the structural stability of the electrode, enhance the reversible capacity and working voltage of the full cell and reduce the resistance, which thus increases the energy and power densities and cycling life. However, current pre-lithiation technologies such as internal or external short circuit [67][68] or using lithium-containing compounds [69][70][71] are either unsafe, time-consuming or inefficient. Hence, high-efficiency pre-lithiation methods are highly needed. Benefiting from well-developed LIBs and SCs, the design strategies, assembly technology and components (conductive additives, binders and shell) could be easily transferred to LICs [72]. More importantly, special attention should be given to thermal management, which is exceptionally critical for the safe and efficient operation of LICs, especially at high and low temperatures [73].
- (8) Additionally, considering the limited and uneven distribution of lithium resources, other metal-ion capacitors are drawing increasing attention and have recently become the research hotspot. In particular, monovalent ion systems (i.e., sodium-ion capacitors and potassium-ion capacitors) are the most promising alternatives to LICs because they have a similar cell configuration and energy storage mechanism as well as abundant resources [74][75]. However, like LICs, Na/K-ion capacitors also suffer from safety problems derived from the use of organic electrolytes and the formation of highly reactive metal dendrites. Recently, multivalent ion systems are drawing more interest due to the merits of providing twice or triple the amount of electrons per unit of active materials as well as being less sensitive to air and water, rendering them low-cost, high-energy and safe devices [76][77]. These novel systems are still in the early stage and more efforts should be devoted to preparing advanced electrode materials, developing suitable electrolytes and investigating the energy storage mechanism.

In conclusion, LICs have witnessed tremendous progress during the last decade, especially in electrode materials. Their development steps are speeding up and large-scale application will be realized in the near future. Without a

doubt, graphene-based nanomaterials could play a vital role in achieving high performance due to their outstanding electrochemical properties.

---

## References

1. Zheng, S.; Wu, Z.-S.; Wang, S.; Xiao, H.; Zhou, F.; Sun, C.; Bao, X.; Cheng, H.-M. Graphene-based materials for high-voltage and high-energy asymmetric supercapacitors. *Energy Storage Mater.* 2017, 6, 70–97.
2. Mahmood, N.; Zhang, C.; Yin, H.; Hou, Y. Graphene-based nanocomposites for energy storage and conversion in lithium batteries, supercapacitors and fuel cells. *J. Mater. Chem. A* 2014, 2, 15–32.
3. Petnikota, S.; Rotte, N.K.; Srikanth, V.V.S.S.; Kota, B.S.R.; Reddy, M.V.; Loh, K.P.; Chowdari, B.V.R. Electrochemical studies of few-layered graphene as an anode material for Li ion batteries. *J. Solid State Electrochem.* 2014, 18, 941–949.
4. Goh, B.-M.; Wang, Y.; Reddy, M.V.; Ding, Y.L.; Lu, L.; Bunker, C.; Loh, K.P. Filling the Voids of Graphene Foam with Graphene “Eggshell” for Improved Lithium-Ion Storage. *ACS Appl. Mater. Interfaces* 2014, 6, 9835–9841.
5. Zhang, M.; Sun, Z.; Zhang, T.; Qin, B.; Sui, D.; Xie, Y.; Ma, Y.; Chen, Y. Porous asphalt/graphene composite for supercapacitors with high energy density at superior power density without added conducting materials. *J. Mater. Chem. A* 2017, 5, 21757–21764.
6. Ma, Y.; Chang, H.; Zhang, M.; Chen, Y. Graphene-Based Materials for Lithium-Ion Hybrid Supercapacitors. *Adv. Mater.* 2015, 27, 5296–5308.
7. Su, F.; Hou, X.; Qin, J.; Wu, Z.-S. Recent Advances and Challenges of Two-Dimensional Materials for High-Energy and High-Power Lithium-Ion Capacitors. *Batter. Supercaps* 2020, 3, 10–29.
8. Wang, Y.; Wu, Y.; Huang, Y.; Zhang, F.; Yang, X.; Ma, Y.; Chen, Y. Preventing Graphene Sheets from Restacking for High-Capacitance Performance. *J. Phys. Chem. C* 2011, 115, 23192–23197.
9. Han, D.; Zhang, J.; Weng, Z.; Kong, D.; Tao, Y.; Ding, F.; Ruan, D.; Yang, Q.-H. Two-dimensional materials for lithium/sodium-ion capacitors. *Mater. Today Energy* 2019, 11, 30–45.
10. Lang, J.; Zhang, X.; Liu, B.; Wang, R.; Chen, J.; Yan, X. The roles of graphene in advanced Li-ion hybrid supercapacitors. *J. Energy Chem.* 2018, 27, 43–56.
11. Li, C.; Zhang, X.; Sun, C.; Wang, K.; Sun, X.; Ma, Y. Recent progress of graphene-based materials in lithium-ion capacitors. *J. Phys. D Appl. Phys.* 2019, 52, 143001.

12. Zhang, L.; Liang, J.; Huang, Y.; Ma, Y.; Wang, Y.; Chen, Y. Size-controlled synthesis of graphene oxide sheets on a large scale using chemical exfoliation. *Carbon* 2009, 47, 3365–3368.
13. Tu, F.; Liu, S.; Wu, T.; Jin, G.; Pan, C. Porous graphene as cathode material for lithium ion capacitor with high electrochemical performance. *Powder Technol.* 2014, 253, 580–583.
14. Lee, J.H.; Shin, W.H.; Ryou, M.-H.; Jin, J.K.; Kim, J.; Choi, J.W. Functionalized Graphene for High Performance Lithium Ion Capacitors. *ChemSusChem* 2012, 5, 2328–2333.
15. Sui, D.; Xu, L.; Zhang, H.; Sun, Z.; Kan, B.; Ma, Y.; Chen, Y. A 3D cross-linked graphene-based honeycomb carbon composite with excellent confinement effect of organic cathode material for lithium-ion batteries. *Carbon* 2020, 157, 656–662.
16. Wu, M.; Zhao, Y.; Sun, B.; Sun, Z.; Li, C.; Han, Y.; Xu, L.; Ge, Z.; Ren, Y.; Zhang, M.; et al. A 2D covalent organic framework as a high-performance cathode material for lithium-ion batteries. *Nano Energy* 2020, 70, 104498.
17. Aravindan, V.; Mhamane, D.; Ling, W.C.; Ogale, S.; Madhavi, S. Nonaqueous Lithium-Ion Capacitors with High Energy Densities using Trigol-Reduced Graphene Oxide Nanosheets as Cathode-Active Material. *ChemSusChem* 2013, 6, 2240–2244.
18. Wang, H.; Guan, C.; Wang, X.; Fan, H.J. A High Energy and Power Li-Ion Capacitor Based on a TiO<sub>2</sub> Nanobelt Array Anode and a Graphene Hydrogel Cathode. *Small* 2015, 11, 1470–1477.
19. Ye, L.; Liang, Q.; Lei, Y.; Yu, X.; Han, C.; Shen, W.; Huang, Z.-H.; Kang, F.; Yang, Q.-H. A high performance Li-ion capacitor constructed with Li<sub>4</sub>Ti<sub>5</sub>O<sub>12</sub>/C hybrid and porous graphene macroform. *J. Power Sources* 2015, 282, 174–178.
20. Li, H.; Shen, L.; Wang, J.; Fang, S.; Zhang, Y.; Dou, H.; Zhang, X. Three-dimensionally ordered porous TiNb<sub>2</sub>O<sub>7</sub> nanotubes: A superior anode material for next generation hybrid supercapacitors. *J. Mater. Chem. A* 2015, 3, 16785–16790.
21. Wu, Y.; Yi, N.; Huang, L.; Zhang, T.; Fang, S.; Chang, H.; Li, N.; Oh, J.; Lee, J.A.; Kozlov, M.; et al. Three-dimensionally bonded spongy graphene material with super compressive elasticity and near-zero Poisson's ratio. *Nat. Commun.* 2015, 6, 6141.
22. Dubal, D.P.; Gomez-Romero, P. All nanocarbon Li-Ion capacitor with high energy and high power density. *Mater. Today Energy* 2018, 8, 109–117.
23. Sha, J.; Chu, X.; Xu, T.; Li, Y.; Tang, Y.; Ma, L.; Shi, C.; Liu, E.; Zhao, D.; He, C.; et al. Bi-functional modular graphene network with high rate and cycling performance. *J. Power Sources* 2021, 504, 230075.
24. Jin, L.; Guo, X.; Gong, R.; Zheng, J.; Xiang, Z.; Zhang, C.; Zheng, J.P. Target-oriented electrode constructions toward ultra-fast and ultra-stable all-graphene lithium ion capacitors. *Energy Storage Mater.* 2019, 23, 409–417.

25. Ma, X.; Gao, D. High Capacitive Storage Performance of Sulfur and Nitrogen Codoped Mesoporous Graphene. *ChemSusChem* 2018, 11, 1048–1055.
26. Fan, Q.; Yang, M.; Meng, Q.; Cao, B.; Yu, Y. Activated-Nitrogen-Doped Graphene-Based Aerogel Composites as Cathode Materials for High Energy Density Lithium-Ion Supercapacitor. *J. Electrochem. Soc.* 2016, 163, A1736–A1742.
27. Wang, J.; Kaskel, S. KOH activation of carbon-based materials for energy storage. *J. Mater. Chem.* 2012, 22, 23710–23725.
28. Zhu, Y.; Murali, S.; Stoller, M.D.; Ganesh, K.J.; Cai, W.; Ferreira, P.J.; Pirkle, A.; Wallace, R.M.; Cychosz, K.A.; Thommes, M.; et al. Carbon-Based Supercapacitors Produced by Activation of Graphene. *Science* 2011, 332, 1537–1541.
29. Stoller, M.D.; Murali, S.; Quarles, N.; Zhu, Y.; Potts, J.R.; Zhu, X.; Ha, H.-W.; Ruoff, R.S. Activated graphene as a cathode material for Li-ion hybrid supercapacitors. *Phys. Chem. Chem. Phys.* 2012, 14, 3388–3391.
30. Li, Y.; Wang, R.; Zheng, W.; Zhao, Q.; Sun, S.; Ji, G.; Li, S.; Fan, X.; Xu, C. Design of Nb<sub>2</sub>O<sub>5</sub>/graphene hybrid aerogel as polymer binder-free electrodes for lithium-ion capacitors. *Mater. Technol.* 2020, 35, 625–634.
31. Yang, Y.; Lin, Q.; Ding, B.; Wang, J.; Malgras, V.; Jiang, J.; Li, Z.; Chen, S.; Dou, H.; Alshehri, S.M.; et al. Lithium-ion capacitor based on nanoarchitected polydopamine/graphene composite anode and porous graphene cathode. *Carbon* 2020, 167, 627–633.
32. Jeong, J.H.; Lee, G.-W.; Kim, Y.H.; Choi, Y.J.; Roh, K.C.; Kim, K.-B. A holey graphene-based hybrid supercapacitor. *Chem. Eng. J.* 2019, 378, 122126.
33. Zhang, L.; Zhang, F.; Yang, X.; Long, G.; Wu, Y.; Zhang, T.; Leng, K.; Huang, Y.; Ma, Y.; Yu, A.; et al. Porous 3D graphene-based bulk materials with exceptional high surface area and excellent conductivity for supercapacitors. *Sci. Rep.* 2013, 3, 1408.
34. Zhang, F.; Zhang, T.; Yang, X.; Zhang, L.; Leng, K.; Huang, Y.; Chen, Y. A high-performance supercapacitor-battery hybrid energy storage device based on graphene-enhanced electrode materials with ultrahigh energy density. *Energy Environ. Sci.* 2013, 6, 1623–1632.
35. Dai, X.; Lei, S.; Liu, J.; Shang, Z.; Zhong, S.; Li, X. Promoting the energy density of lithium-ion capacitor by coupling the pore-size and nitrogen content in capacitive carbon cathode. *J. Power Sources* 2021, 498, 229912.
36. Yang, J.; Xu, D.; Hou, R.; Lang, J.; Wang, Z.; Dong, Z.; Ma, J. Nitrogen-doped carbon nanotubes by multistep pyrolysis process as a promising anode material for lithium ion hybrid capacitors. *Chin. Chem. Lett.* 2020, 31, 2239–2244.

37. Salvatierra, R.V.; Zakhidov, D.; Sha, J.; Kim, N.D.; Lee, S.-K.; Raji, A.-R.O.; Zhao, N.; Tour, J.M. Graphene Carbon Nanotube Carpets Grown Using Binary Catalysts for High-Performance Lithium-Ion Capacitors. *ACS Nano* 2017, 11, 2724–2733.
38. Li, N.-W.; Du, X.; Shi, J.-L.; Zhang, X.; Fan, W.; Wang, J.; Zhao, S.; Liu, Y.; Xu, W.; Li, M.; et al. meso-/microporous carbon for ultrahigh energy density lithium-ion capacitors. *Electrochim. Acta* 2018, 281, 459–465.
39. Li, P.; Li, H.; Han, D.; Shang, T.; Deng, Y.; Tao, Y.; Lv, W.; Yang, Q.-H. Packing Activated Carbons into Dense Graphene Network by Capillarity for High Volumetric Performance Supercapacitors. *Adv. Sci.* 2019, 6, 1802355.
40. Wang, J.-A.; Li, S.-M.; Wang, Y.-S.; Lan, P.-Y.; Liao, W.-H.; Hsiao, S.-T.; Lin, S.-C.; Lin, C.-W.; Ma, C.-C.M.; Hu, C.-C. Preparation and Properties of NrGO-CNT Composite for Lithium-Ion Capacitors. *J. Electrochem. Soc.* 2017, 164, A3657–A3665.
41. Adelowo, E.; Baboukani, A.R.; Chen, C.; Wang, C. Electrostatically Sprayed Reduced Graphene Oxide-Carbon Nanotubes Electrodes for Lithium-Ion Capacitors. *C* 2018, 4, 31.
42. Li, B.; Zhang, H.; Zhang, C. Agricultural waste-derived activated carbon/graphene composites for high performance lithium-ion capacitors. *RSC Adv.* 2019, 9, 29190–29194.
43. Wang, X.; Wang, Z.; Zhang, X.; Peng, H.; Xin, G.; Lu, C.; Zhong, Y.; Wang, G.; Zhang, Y. Nitrogen-Doped Defective Graphene Aerogel as Anode for all Graphene-Based Lithium Ion Capacitor. *ChemistrySelect* 2017, 2, 8436–8445.
44. Liu, Y.; Wang, W.; Chen, J.; Li, X.; Cheng, Q.; Wang, G. Fabrication of porous lithium titanate self-supporting anode for high performance lithium-ion capacitor. *J. Energy Chem.* 2020, 50, 344–350.
45. Sun, Y.; Tang, J.; Qin, F.; Yuan, J.; Zhang, K.; Li, J.; Zhu, D.-M.; Qin, L.-C. Hybrid lithium-ion capacitors with asymmetric graphene electrodes. *J. Mater. Chem. A* 2017, 5, 13601–13609.
46. Yang, H.; Kannappan, S.; Pandian, A.S.; Jang, J.-H.; Lee, Y.S.; Lu, W. Graphene supercapacitor with both high power and energy density. *Nanotechnology* 2017, 28, 445401.
47. Yu, X.; Zhan, C.; Lv, R.; Bai, Y.; Lin, Y.; Huang, Z.-H.; Shen, W.; Qiu, X.; Kang, F. Ultrahigh-rate and high-density lithium-ion capacitors through hybridizing nitrogen-enriched hierarchical porous carbon cathode with prelithiated microcrystalline graphite anode. *Nano Energy* 2015, 15, 43–53.
48. Han, D.; Weng, Z.; Li, P.; Tao, Y.; Cui, C.; Zhang, L.; Lin, W.; Gao, Y.; Kong, D.; Yang, Q.-H. Electrode thickness matching for achieving high-volumetric-performance lithium-ion capacitors. *Energy Storage Mater.* 2019, 18, 133–138.
49. Zhang, L.; Yang, X.; Zhang, F.; Long, G.; Zhang, T.; Leng, K.; Zhang, Y.; Huang, Y.; Ma, Y.; Zhang, M.; et al. Controlling the Effective Surface Area and Pore Size Distribution of sp<sup>2</sup> Carbon

- Materials and Their Impact on the Capacitance Performance of These Materials. *J. Am. Chem. Soc.* 2013, 135, 5921–5929.
50. Tie, D.; Huang, S.; Wang, J.; Ma, J.; Zhang, J.; Zhao, Y. Hybrid energy storage devices: Advanced electrode materials and matching principles. *Energy Storage Mater.* 2019, 21, 22–40.
51. Liu, B.; Chen, J.; Yang, B.; Liu, L.; Sun, Y.; Hou, R.; Lin, Z.; Yan, X. Boosting the performance of lithium metal capacitors with a Li composite anode. *J. Mater. Chem. A* 2021, 9, 10722–10730.
52. Guo, F.; Wu, C.; Chen, H.; Zhong, F.; Ai, X.; Yang, H.; Qian, J. Dendrite-free lithium deposition by coating a lithiophilic heterogeneous metal layer on lithium metal anode. *Energy Storage Mater.* 2020, 24, 635–643.
53. Luo, D.; Li, M.; Zheng, Y.; Ma, Q.; Gao, R.; Zhang, Z.; Dou, H.; Wen, G.; Shui, L.; Yu, A.; et al. Electrolyte Design for Lithium Metal Anode-Based Batteries Toward Extreme Temperature Application. *Adv. Sci.* 2021, 8, 2101051.
54. Zong, J.; Ni, W.; Xu, H.; Ding, F.; Wang, T.; Feng, W.; Liu, X. High tap-density graphene cathode material for lithium-ion capacitors via a mass-scalable synthesis method. *Chem. Eng. J.* 2019, 360, 1233–1240.
55. Hirota, N.; Okuno, K.; Majima, M.; Hosoe, A.; Uchida, S.; Ishikawa, M. High-performance lithium-ion capacitor composed of electrodes with porous three-dimensional current collector and bis(fluorosulfonyl)imide-based ionic liquid electrolyte. *Electrochim. Acta* 2018, 276, 125–133.
56. Dou, Q.; Wang, Y.; Wang, A.; Ye, M.; Hou, R.; Lu, Y.; Su, L.; Shi, S.; Zhang, H.; Yan, X. “Water in salt/ionic liquid” electrolyte for 2.8 V aqueous lithium-ion capacitor. *Sci. Bull.* 2020, 65, 1812–1822.
57. Tian, X.; Zhu, Q.; Xu, B. “Water-in-Salt” Electrolytes for Supercapacitors: A Review. *ChemSusChem* 2021, 14, 2501–2515.
58. Shen, Y.; Liu, B.; Liu, X.; Liu, J.; Ding, J.; Zhong, C.; Hu, W. Water-in-salt electrolyte for safe and high-energy aqueous battery. *Energy Storage Mater.* 2021, 34, 461–474.
59. Dong, S.; Wang, Y.; Chen, C.; Shen, L.; Zhang, X. Niobium Tungsten Oxide in a Green Water-in-Salt Electrolyte Enables Ultra-Stable Aqueous Lithium-Ion Capacitors. *Nano-Micro Lett.* 2020, 12, 168.
60. Qin, H.; Chao, H.; Zhang, M.; Huang, Y.; Liu, H.; Cheng, J.; Cao, L.; Xu, Q.; Guan, L.; Teng, X.; et al. Precious potential regulation of carbon cathode enabling high-performance lithium-ion capacitors. *Carbon* 2021, 180, 110–117.
61. Shan, X.-Y.; Wang, Y.; Wang, D.-W.; Li, F.; Cheng, H.-M. Armoring Graphene Cathodes for High-Rate and Long-Life Lithium Ion Supercapacitors. *Adv. Energy Mater.* 2016, 6, 1502064.

62. Yousaf, M.; Naseer, U.; Li, Y.; Ali, Z.; Mahmood, N.; Wang, L.; Gao, P.; Guo, S. A mechanistic study of electrode materials for rechargeable batteries beyond lithium ions by in situ transmission electron microscopy. *Energy Environ. Sci.* 2021, 14, 2670–2707.
63. Gbadamasi, S.; Mohiuddin, M.; Krishnamurthi, V.; Verma, R.; Khan, M.W.; Pathak, S.; Kalantar-Zadeh, K.; Mahmood, N. Interface chemistry of two-dimensional heterostructures – fundamentals to applications. *Chem. Soc. Rev.* 2021, 50, 4684–4729.
64. Jian, X.; Wang, H.; Rao, G.; Jiang, L.; Wang, H.; Subramaniam, C.M.; Mahmood, A.; Zhang, W.; Xiang, Y.; Dou, S.X.; et al. Self-tunable ultrathin carbon nanocups as the electrode material of sodium-ion batteries with unprecedented capacity and stability. *Chem. Eng. J.* 2019, 364, 578–588.
65. Jin, L.; Shen, C.; Shellikeri, A.; Wu, Q.; Zheng, J.; Andrei, P.; Zhang, J.-G.; Zheng, J.P. Progress and perspectives on pre-lithiation technologies for lithium ion capacitors. *Energy Environ. Sci.* 2020, 13, 2341–2362.
66. Rao, Z.; Wu, J.; He, B.; Chen, W.; Wang, H.; Fu, Q.; Huang, Y. A Prelithiation Separator for Compensating the Initial Capacity Loss of Lithium-Ion Batteries. *ACS Appl. Mater. Interfaces* 2021, 13, 38194–38201.
67. Sivakkumar, S.R.; Pandolfo, A.G. Evaluation of lithium-ion capacitors assembled with pre-lithiated graphite anode and activated carbon cathode. *Electrochim. Acta* 2012, 65, 280–287.
68. Kim, M.; Xu, F.; Lee, J.H.; Jung, C.; Hong, S.M.; Zhang, Q.M.; Koo, C.M. A fast and efficient pre-doping approach to high energy density lithium-ion hybrid capacitors. *J. Mater. Chem. A* 2014, 2, 10029–10033.
69. Jeżowski, P.; Crosnier, O.; Deunf, E.; Poizot, P.; Béguin, F.; Brousse, T. Safe and recyclable lithium-ion capacitors using sacrificial organic lithium salt. *Nat. Mater.* 2018, 17, 167–173.
70. Park, M.-S.; Lim, Y.-G.; Hwang, S.M.; Kim, J.H.; Kim, J.-S.; Dou, S.X.; Cho, J.; Kim, Y.-J. Scalable Integration of Li<sub>5</sub>FeO<sub>4</sub> towards Robust, High-Performance Lithium-Ion Hybrid Capacitors. *ChemSusChem* 2014, 7, 3138–3144.
71. Liu, C.; Li, T.; Zhang, H.; Song, Z.; Qu, C.; Hou, G.; Zhang, H.; Ni, C.; Li, X. DMF stabilized Li<sub>3</sub>N slurry for manufacturing self-prelithiatable lithium-ion capacitors. *Sci. Bull.* 2020, 65, 434–442.
72. An, Y.; Liu, T.; Li, C.; Zhang, X.; Hu, T.; Sun, X.; Wang, K.; Wang, C.; Ma, Y. A general route for the mass production of graphene-enhanced carbon composites toward practical pouch lithium-ion capacitors. *J. Mater. Chem. A* 2021, 9, 15654–15664.
73. Karimi, D.; Khaleghi, S.; Behi, H.; Beheshti, H.; Hosen, M.S.; Akbarzadeh, M.; Van Mierlo, J.; Berecibar, M. Lithium-Ion Capacitor Lifetime Extension through an Optimal Thermal Management System for Smart Grid Applications. *Energies* 2021, 14, 2907.

74. Zhang, Y.; Jiang, J.; An, Y.; Wu, L.; Dou, H.; Zhang, J.; Zhang, Y.; Wu, S.; Dong, M.; Zhang, X.; et al. Sodium-ion capacitors: Materials, Mechanism, and Challenges. *ChemSusChem* 2020, 13, 2522–2539.
75. Liu, M.; Chang, L.; Le, Z.; Jiang, J.; Li, J.; Wang, H.; Zhao, C.; Xu, T.; Nie, P.; Wang, L. Emerging Potassium-ion Hybrid Capacitors. *ChemSusChem* 2020, 13, 5837–5862.
76. Ma, X.; Cheng, J.; Dong, L.; Liu, W.; Mou, J.; Zhao, L.; Wang, J.; Ren, D.; Wu, J.; Xu, C.; et al. Multivalent ion storage towards high-performance aqueous zinc-ion hybrid supercapacitors. *Energy Storage Mater.* 2019, 20, 335–342.
77. Sui, D.; Wu, M.; Shi, K.; Li, C.; Lang, J.; Yang, Y.; Zhang, X.; Yan, X.; Chen, Y. Recent progress of cathode materials for aqueous zinc-ion capacitors: Carbon-based materials and beyond. *Carbon* 2021, 185, 126–151.
- 

Retrieved from <https://encyclopedia.pub/entry/history/show/40426>